Shahrood University of Technology

Journal of Mining and Environment (JME)

Journal homepage: www.jme.shahroodut.ac.ir

Iranian Society of Mining Engineering (IRSME)

Application of Hybrid Wavelet-Fractal Approach for Denoising and Spatial Modeling of Environmental Pollution

Hossein Mahdiyanfar[1], and Mir Mahdi Seyedrahimi-Niaraq[2]*

1. Department of Mining Engineering, University of Gonabad, Gonabad, Iran
2. Department of Mining Engineering, Faculty of Engineering, University of Mohaghegh Ardabili, Ardabil, Iran

Article Info

Received 15 February 2024
Received in Revised form 12 April 2024
Accepted 3 June 2024
Published online 3 June 2024

DOI: 10.22044/jme.2024.14197.2643

Keywords

Wavelet transformation
Symlet and Haar wavelet
Concentration-area fractal
Wavelet-Fractal model
Environmental pollution

Abstract

In this investigation, the hybrid approach of wavelet transforms and fractal method named Wavelet-Fractal model has been utilized for geochemical contamination mapping as a novel application. For this purpose, the distribution maps of pollutant elements were transformed to the position-scale domain using two-dimensional discrete wavelet transformation (2DDWT). The Symlet2 and Haar mother wavelets were applied for two-dimensional signal analysis of elemental concentrations of As, Pb, and Zn based on soil samples taken from the Irankuh mining district, Central Iran. The Symlet2 and Haar wavelet coefficients of approximate and detail components were obtained at one level frequency decomposition using 2DDWT. The wavelet coefficients of approximate component (WCAC) were modeled using a fractal method for delineating the geochemical contamination populations of toxic elements. Based on the results of wavelet-fractal models, the As, pb, and Zn were classified into three and four populations. Two areas contaminated with metals have been found in the district. These areas are within the limit of mining operations and its surroundings. The wavelet-fractal proposed model has been able to separate environmental areas contaminated with toxic metals accurately. Anomalously intense pollution has spread to one kilometer outside the mining operation limit. This dispersion in the case of Pb and Zn elements is well seen in the geochemical map prepared with the Haar class.

1. Introduction

Pollution can destroy the environment, wildlife, and human health. Pollution control efforts include air pollution control, wastewater treatment, solid-waste management, hazardous-waste management, and recycling. Pollutants can be natural or human-made, such as, mining activities, volcanic ash or trash produced by factories. The significant types of pollution are air pollution, water pollution, and land pollution [1,2]. Pollution has widespread wrecking impacts on the environment, and growing evidence of local and global pollution has attracted attention [3,4]. There are environmental concerns about the effects of mining activities specially include extraction operations, dumping waste, waste dam and mineral processing phases. These activities spread heavy elements in the surrounding areas, hence the evaluation of the amount of contamination caused by heavy and toxic elements and delineation of contaminated areas are essential subjects in environmental geochemistry [5-7]. Contamination mapping is the essential stage for constructing maps that illustrate the positions of contaminated locations, pollution sources, and impacts on surrounding districts. These created maps are suitable tools for understanding the contamination dispersion type in various areas and can be utilized for pollution controlling and decision making about remediation ways [8-10].

Various approaches have been presented for geochemical mapping to explore mineral ore deposits or detect the geochemical environmental pollution regions [11-13]. The geochemical populations can be distinguished and the spatial exploratory or pollution evidences can be

Corresponding author: M.seyedrahimi@uma.ac.ir (M.M. Seyedrahimi-Niaraq)

highlighted using geochemical mapping approaches. The geochemical exploratory maps are delineated using various mathematical approaches in the spatial domain, frequency domain [13-15], and wavelet domain [16-18]. Fractal theory is a common way to separate geochemical populations and have been widely performed in geochemistry to model complex mineralization and geological phenomena. Fractal analysis has been utilized for interpretation of various fields, such as exploratory and environmental geochemistry. These models have been applied to various geochemical data and have shown promise in understanding the underlying patterns and processes in this field [19-24]. The fractal theory has been applied to model geochemical dataset in spatial, frequency, and wavelet domains. The DWT has high ability to acquire precise and significant results for various data processing. It has been applied in various science fields, such as image processing and data analysis [25]. The wavelet-base fractal method is a new approach used in geochemical exploration field for anomaly separation [26, 27]. In some new researches, the integrated method has been used to separate geochemical potential areas [28, 29]. In this study, the Wavelet-Fractal method was used for modeling of the environmental geochemical dataset and recognizing the pollution patterns as a novel application. The wavelet transform is a mathematical technique performed for data processing and analysis. The advantage of the wavelet transform over the Fourier transform is that the frequency and time (or location) components are considered together. The high and low-frequency components of spatial or temporal signals are distinguished using the wavelet transform. The wavelet transform can be implemented through a convolution of a signal and a wavelet function, and it presents the exciting information about the scale and frequency features of dataset [30-36].

2. Case study and data

The study area is located near the Irankuh mountain limit in Isfahan province. This area has Irankuh lead and zinc mine, located in the metamorphic rocks of Sanandaj-Sirjan zone. This zone is considered a unit of Zagros orogeny in the west of Iran [37, 38]. The mineralization type of Irankuh mine as a Pb-Zn epigenetic deposit is Mississippi Valley-type, and its host rocks include limited Jurassic shale and lower Cretaceous dolostone. The replacement process has caused lead and zinc mineralization within dolomite and shale rocks. This process is manifested in the form of breccia, veinlets, and filled space [39]. There are several styles of mineralization in the study area, such as sulphide mineralization whose constituents are massive and semi-massive, brecciated, laminated, vein-veinlet, disseminated, colloform and framboidal. Another style of hydrothermal mineralization is associated with hydrothermal alteration such as dolomitization, silicification and sericitization. Non-sulfide mineralization in the area can be referred to as supergene mineralization [40]. The faults and fractured zones control the orebodies, and the Pb-Zn hydrothermal mineralization is shown in these structures and has created alterations of dolomitization and silicification. Sphalerite and dolomite rich in iron and manganese, ankrite, galena, bituminous, pyrite and calcite ± quartz ± barite are the main minerals of the region. The climate of the area is semi-arid, and it is windy from March to May and sometimes from September to October [41]. The composition of the soils of the area is calcic, organic compounds with low salt, and has a pH of about 7 to 8. The amount of sand, silt and clay is about 44, 39 and 17, respectively [42, 43]. The areas near the mine have plants and agricultural products contaminated with heavy metals containing lead and zinc. These metals are dispersed through dust. For this reason, it has caused environmental concerns for agricultural purposes [44].

The geological map of the study area is shown in Figure 1. On this Figure, the location of 137 soil samples taken from a depth of 0 to 30 cm in industrial, residential and mainly agricultural backgrounds is also given. The sampling network was designed based on a systematic grid with an interval of 500 m. The samples were analyzed for 44 elements consisting of heavy metals using ICP-OES. Studying the relationship between geochemical contaminant elements and their pattern shows that the leading cause of element dispersion around the mining site is dust [43, 45].

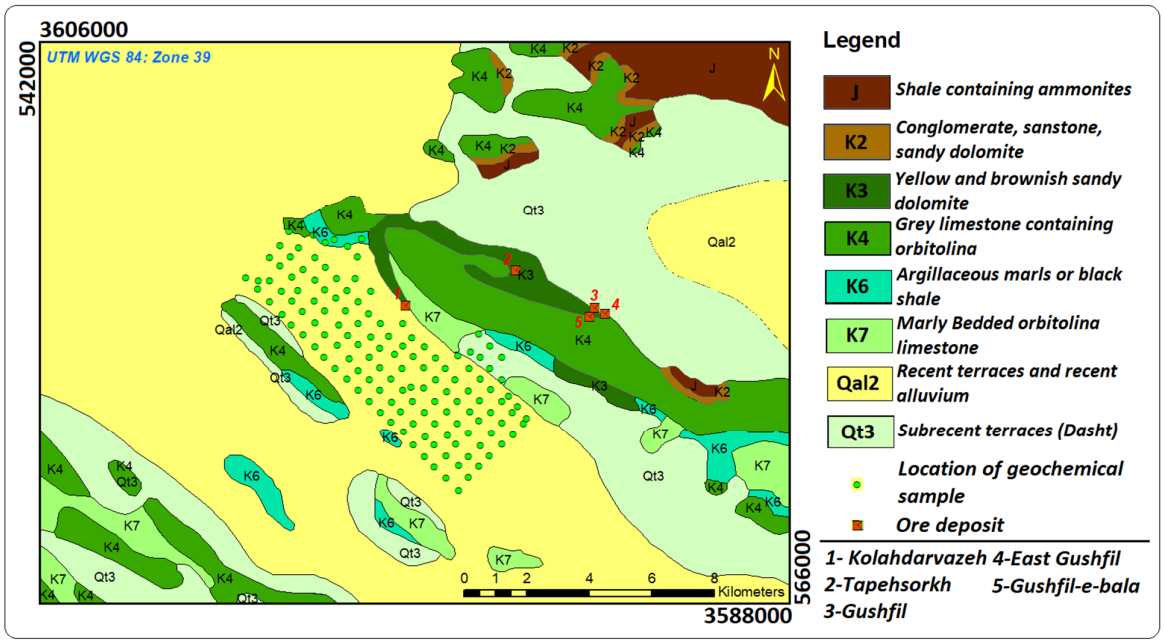

Figure 1. Geological map of the study area. The locations of the soil samples are shown with green circles.

3. Methodology

3.1. Wavelet analysis

Wavelet transformation and related theoretical topics were widely developed in the middle of the 18th century in various sciences [46]. The wavelet transform, $W_x(a, b)$, of a continuous temporal or spatial signal, x(t), is defined as follows:

$$w_x(a,b) = \frac{1}{\sqrt{a}} \int_{-\infty}^{+\infty} x(t)\psi^*\left(\frac{t-b}{a}\right)dt \qquad (1)$$

$$(a,b) \in R^2$$

Therefore, the wavelet transform is calculated by the internal multiplication of x(t) and the transferred and scaled version of the single function ψ (t), which is called the wavelet [42]. By changing the scaling parameter of a, the frequency center and the bandwidth of the interpass are affected. Temporal and frequency resolution depends on the parameter of a. For analysis of high frequencies (low a), time localization is suitable, but frequency resolution is low. On the other hand, for the analysis of low frequencies, super frequency resolution and low time resolution will be obtained. The time transition is done by the changing of the parameter b. Wavelet analysis is often called time-scale analysis instead of time-frequency analysis [47]. The wavelet coefficients depend on the values of a and b. In discrete wavelet transformation, discrete values of a and b are used, and their values are considered as follows [48].

$$a = 2^j \qquad b = k2^j \quad , \quad k, j \in Z^2 \qquad (2)$$

Wavelet analysis can be used to decompose the signal into detail and approximate components. The primary temporal or spatial signal is passed through two high and low pass filters. The detailed approximate components are obtained using high-pass and low-pass filtering, respectively. Therefore, the initial signal in the temporal or spatial domain can be decomposed and investigated in different resolutions. Different resolutions are created due to different scales and contain different information [48]. In the DWT method, the signal x is decomposed into two high and low frequency parts in the first step, and in the second step, the low frequency part is again divided into two high and low frequency components. This can continue to various stages of filtering [49]. The wavelet analysis can extract information from data at different scales and be used as a powerful tool in data processing due to its multi-resolution nature. Partial information in the field of location or time and frequency simultaneously can be analyzed in the wavelet method and increase the accuracy of the analysis, so the wavelet method is more flexible than the Fourier analysis method. The two-dimensional discrete wavelet method decomposes the primary signal into four components in each step including horizontal detail component, vertical detail component, diagonal detail component and approximate component [50, 51].

The decomposition process of two-dimensional DWT in three levels containing high and low pass filtering has been illustrated in Figure 2. In each decomposition level, signal is divided into detail and approximate parts and in the next decomposition level, the approximate component of previous level is divided. The DWT can generate a sparse signal representation, making it suitable for compression and denoising.

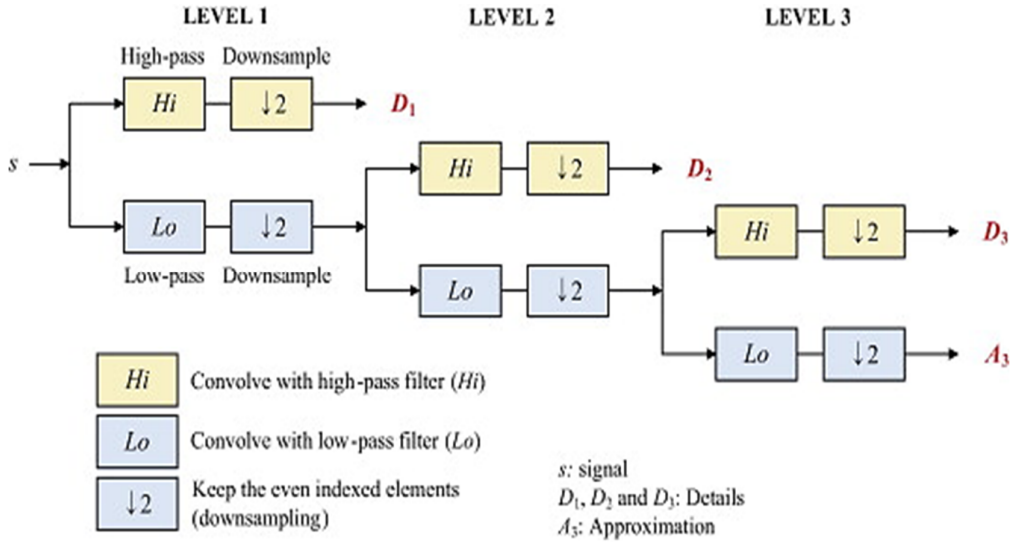

Figure 2. Schematic decomposition of a signal in three levels using two-dimensional DWT [52].

In this study the Symlet2 and Haar mother wavelets were used for geochemical data processing. The Daubechies wavelets are compactly supported orthonormal functions that can be attractively used as DWT of signals. The Daubechies wavelet families have been frequently applied for DWT [53]. The Daubechies wavelet with order1 (named Haar) and order 2 were utilized for geochemical signal processing in this research. These two mentioned mother wavelets conveyed quite similar results hence the results of Haar wavelet were presented in the paper. The signals and functions with speedy transitions can be analyzed by Haar wavelet because of its discontinuity property. The frequency features of functions can be processed using Haar wavelet because of its orthogonal property. The Haar wavelet can be performed for analyzing the localized attribute of functions [53, 54]. The smoothness, regularity and lengthy of filters are the features of Daubechies and symlets wavelets that facilitate the processing of smooth curve and reconstructing the signals. The non-linear signals can be approximated based on these advantages [55, 56]. The Symlets families are proposed by Daubechies based on modified Daubechies wavelets and apply the almost symmetric functions for signal processing. Implementation of the modified wavelets usually present more robustness. These two wavelet families are similar except for the symmetry feature. The Daubechies functions have asymmetric features. The Symlets have been applied for signal processing as a proper tool by researchers [56- 58].

3.2. Fractal modeling of wavelet coefficients

In this research, the advantages of fractal geometry have been used to model wavelet coefficients. This geometry has been used in mineral exploration stages, mainly to separate populations, threshold values, and geochemical anomalies [59-63]. The main problem in this geometry is the fractal dimension. Various methods have been used to calculate fractal dimensions, such as variograms analysis, the area-perimeter relation, concentration-area model, and concentration-distance model [21, 27, 64-66]. In the counter maps of the spatial distribution of elements, if A(ρ) is the counter area with concentration value ρ, its area decreases with increasing concentration [67, 68]. In this case, to define the anomalies and geochemical background, the concentration-area model is as follows:

$$A(\rho)_{(>\rho)} \alpha \rho^{-D} \quad (3)$$

Where A(ρ) is an area with concentration values higher than the contour containing the

concentration value of ρ and D is the exponential feature. In this research, A(ρ) was obtained by counting cells with raw element concentrations. In this method, the cells of the study area are overlapped with a grid. In this case, A(ρ) is obtained by multiplying the area of the cells by the concentrations more significant than the surface. In geochemical explorations, the fractal dimensions associated with anomalies or concentrations related to mineralization will be different from the fractal dimension of the geochemical background, and these anomalies have different power functions of the background value [59]. Therefore, environmental pollution also produces anomalies related to this phenomenon, and its fractal dimension will also differ. This difference results in threshold values and is used in separating anomalous areas. The wavelet coefficients of approximate components (WCAC) can be modeled using fractal methods. In this study, the Symlet2 and Haar wavelet transformations were utilized for mapping of environmental geochemical patterns according to position-scale domain that are used in fractal modeling based on the concentration-area fractal model. In this scenario the WCAC are used instead of concentration and their areas are calculated and the fractal diagram is modeled (WCAC-Area fractal modeling). The WCAC-A fractal model of pollution-related elements was used to classify contamination populations and intensification of environmental geochemical anomalies.

4. Results and discussion

The three-dimensional contour maps of As, Pb and Zn were created using inverse distance squared approach in MATLAB software. These maps were utilized for the 2DDWT method by Symlet2 and Haar mother wavelets. The wavelet functions transform the three-dimensional contoured geochemical signals to the position-scale domain. The spatial elemental geochemical signal is decomposed to four components including horizontal detail, vertical detail, diagnostic detail, and approximate components. The detailed components can be affected by geochemical noises. The denoising of images and signals can be done by removing the details coefficients in 2DDWT. In this study, the geochemical signals of As, Pb, and Zn were decomposed in one level procedure. The wavelet coefficients of detail and approximate components related to original geochemical signals in one decomposition level were calculated for these elements. The coefficients of approximate component are related to fundamental nature of the original elemental signal. The extracted wavelet coefficients convey concordance of the mother wavelet and elemental geochemical maps in various position scales. These coefficients indicate the frequencies of elements in different positions and various scales. Hence, the wavelet coefficient datasets obtained by symlet2 and Haar mother wavelets were investigated as output maps. The coefficients of As, Pb and Zn approximate components denoised from high frequencies were modeled by wavelet-based fractal method. Therefore, wavelet-based fractal modeling was applied to distinguish the thresholds of geochemical populations and separate the environmental anomalies by logarithmic plots.

For the fractal modeling of wavelet coefficients, first, a logarithmic plot of concentration-area was drawn for WCAC data. After statistical analysis of this plot, threshold values for anomalous sub-population were calculated. Firstly, the usual wavelet analysis method was done on the geochemical data, detailed components were removed, and the WCAC was calculated. In the next step, the WCWA scores (Haar and Symlet2) were used as input and modeled by the fractal method. A grid of 85 × 85 m2 (a total of 9500 grids) was considered to estimate the coefficients and interpolate the data using the method of ordinary kriging. This technique was implemented on the wavelet coefficients, and the data was classified. Then, the WCAC-area logarithmic plot was drawn on variables for the three elements of As, Pb, and Zn in two mother wavelets of Haar and Symlet2. These plots are presented in Figure 3. On these graphs, different slopes were identified, representing different populations with different fractal dimensions. Three main populations were detected for the As element in both mother wavelets of Haar and Symlet2. Pb has four primary populations in both wavelets. However, for the Zn element, three populations were identified in Haar and four in Symlet2. Generally, from low to high WCAC values, the fractal dimension increases with different populations. The identified anomalous populations indicate the anthropogenic effects of mining activities. Background populations also have low fractal dimensions and show that these populations have not been affected by mining activities [7, 39, 58, 59]. These fractal dimensions for As, Pb, and Zn elements in two wavelets of Haar and Symlet2 are given in Table 1.

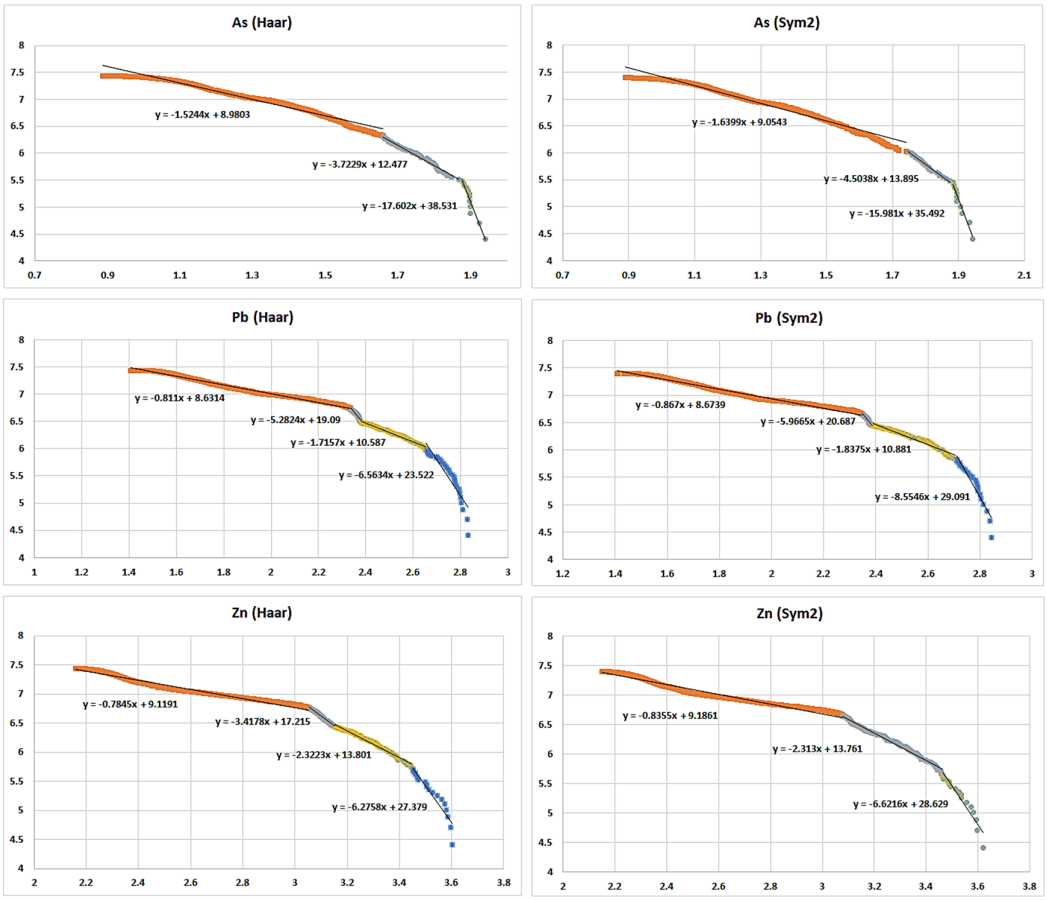

Figure 3. Wavelet-Fractal models of the three elements of As, Pb, and Zn with implementing WCAC-A fractal model of Haar and Symlet2 data

Table 1. Fractal dimensions obtained from primary populations of Wavelet-Fractal models for As, Pb, and Zn in two Haar and Symlet2 wavelets

Element	Haar				Symlet2			
	population 1	population 2	population 3	population 4	population 1	population 2	population 3	population 4
As	1.52	3.72	17.60	-	1.64	4.50	15.98	-
Pb	0.81	5.28	1.72	6.56	0.87	5.97	1.84	8.55
Zn	0.78	3.42	2.32	6.28	0.84	2.31	6.62	-

Figure 4 shows the geochemical maps of As, Pb and Zn elements. These elements are related to pollution. To prepare these maps, first, the concentration-area fractal model was implemented for the wavelet coefficients in Haar and Symlet2 data, and then by separating the separated populations in this model, the maps were provided. The fractal patterns of wavelet coefficients show the limits of estimated populations with different colors on the map. The highest contamination was shown with strong anomaly with jam and red colors. The low limit of strong anomaly for As, Pb and Zn elements is 79, 268 and 1400 respectively in Haar wavelet and 80, 250 and 3000 respectively in Symlet2 wavelet. This pattern changes from yellow with medium anomaly to green background. The distribution maps show that the amount of toxic metals increases by close to the mining site. These elements have a similar increasing pattern, and in high amounts, they show almost the same contaminated areas. To validate the model and identify the source of the contamination, the location of the mining operation limit and the tailings dam are fitted on the final maps (Figure 4). These patterns, which are the results of the Wavelet-Fractal method, show that the mining site is a source of pollution and is spread around the mine with significant dispersion. In agricultural and built-up areas, the concentrations of elements spread to the ground with less intensity.

Two areas contaminated with metals have been found in the area. These areas are within the limit of mining operations and its surroundings. The anomalous pollution intensity is higher for the Pb, followed by the Zn. As is less polluted than the two mentioned elements. Anomalously intense pollution has spread up to one kilometer outside the limit of the mining operation. This dispersion in the case of Pb and Zn elements is well seen in the geochemical map prepared with the Haar class. Also, the pollution in the tailings dam location is intense and extends up to 2 kilometers. In Haar class map, the dispersion of contamination of elements is more than Symlet2 class. The highest populations of zinc and lead have a strong relationship with each other and this relationship is moderate with arsenic element. Various multivariate pollutant indexes were used for identification of pollution areas affected by mining activities. Spatial distribution of toxic elements can be integrated for separating the pollution areas. The applicable scenarios such as principal component analysis, factor analysis, and machine learning algorithms and integrating methods can be utilized for detecting the different pollutant aspects of environments. These multivariate integrated maps and multidimensional views can be useful in decision making process especially about the contaminated agricultural and urban areas.

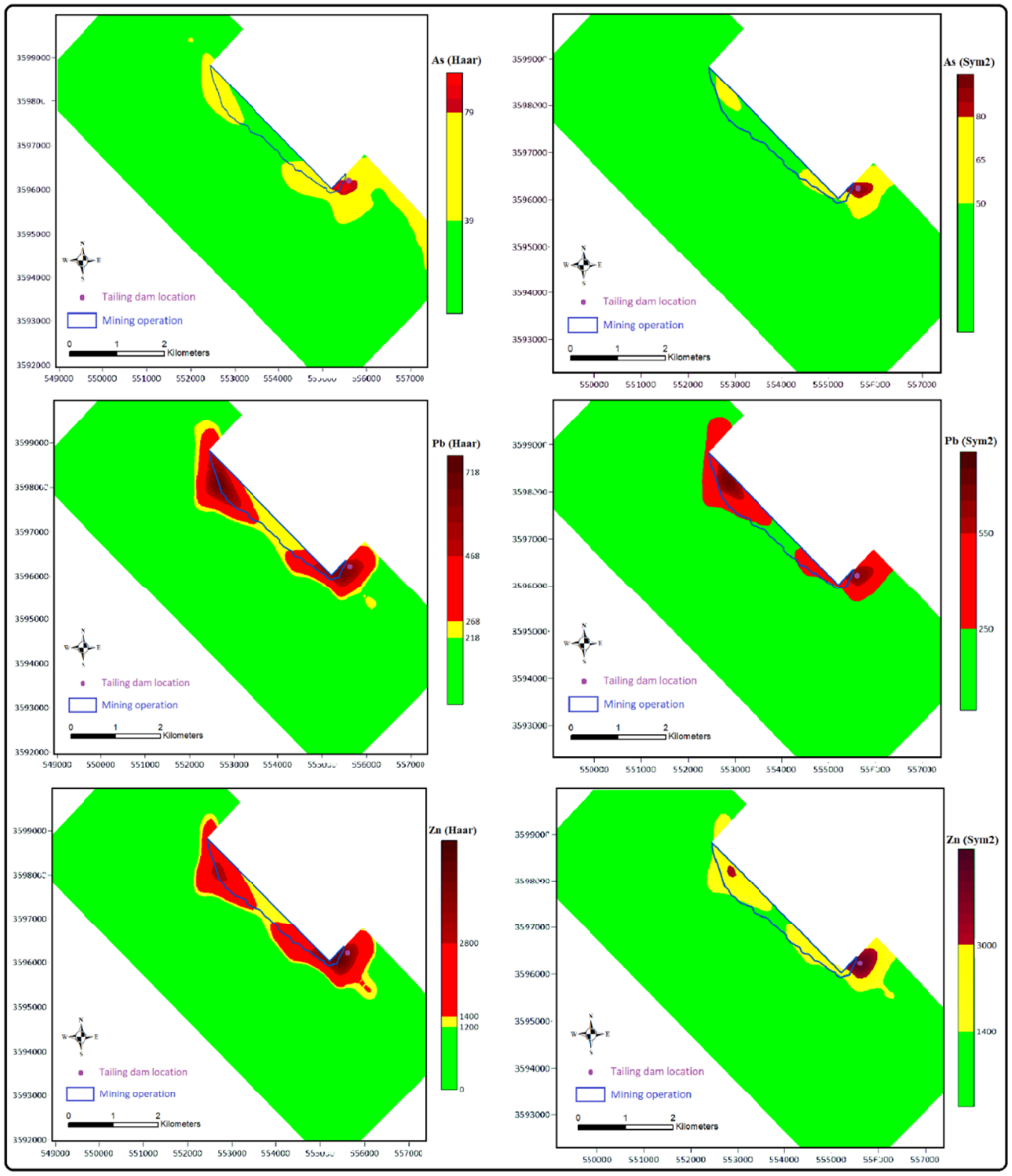

Figure 4 Maps of soil geochemical contamination for arsenic, lead, and iron elements in the Irankuh mining area, obtained by the WCAC-A fractal model.

5. Conclusions

In this investigation, wavelet-fractal modeling was applied to delineate geochemical anomalies of pollutant elements of As, Pb, and Zn in the Irankuh region in the center of Iran. The geochemical denoising of toxic elements was done by eliminating diagonal, horizontal, and vertical detailed components at one level decomposition based on 2DDWT. The Symlet2 and Haar wavelets approximate components were preserved. Their wavelet coefficients for As, Zn, and Pb elements were calculated and modeled using WCAC-A fractal method. The acquired results of wavelet-based fractal modeling indicate that three or four geochemical populations have been separated for As, Pb, and Zn, according to Symlet2 and Haar WCAC. The distribution maps show that the amount of toxic metals increases by close to the mining site. Two areas contaminated with metals have been found in the area. These areas are within the limit of mining operations and its surroundings. The anomalous pollution intensity is higher for the Pb, followed by the Zn. As is less polluted than the two mentioned elements. This dispersion in the case of Pb and Zn elements is well seen in the geochemical map prepared with the Haar class. Also, the pollution in the tailings dam location is intense and extends up to 2 kilometers. In Haar class map, the dispersion of contamination of elements is more than Symlet2 class. The highest populations of zinc and lead have a strong relationship with each other and this relationship is moderate with arsenic element.

Reference

[1]. Ukaogo, P. O., Ewuzie, U., & Onwuka, C. V. (2020). Environmental pollution: causes, effects, and the remedies. *In Microorganisms for sustainable environment and health (pp. 419-429)*. Elsevier.

[2]. Azizi, M., Faz, A., Zornoza, R., Martínez-Martínez, S., Shahrokh, V., & Acosta, J. A. (2022). Environmental pollution and depth distribution of metal (loid) s and rare earth elements in mine tailing. *Journal of Environmental Chemical Engineering, 10(3)*, 107526.

[3]. Bai, Z., Wu, F., He, Y., & Han, Z. (2023). Pollution and risk assessment of heavy metals in Zuoxiguo antimony mining area, southwest China. *Environmental Pollutants and Bioavailability, 35(1)*, 2156397.

[4]. Yu, H., & Zahidi, I. (2023). Environmental hazards posed by mine dust, and monitoring method of mine dust pollution using remote sensing technologies: An overview. *Science of The Total Environment, 864*, 161135.

[5]. Soe, P. S., Kyaw, W. T., Arizono, K., Ishibashi, Y., & Agusa, T. (2022). Mercury pollution from artisanal and small-scale gold mining in Myanmar and other southeast asian countries. *International Journal of Environmental Research and Public Health, 19(10)*, 6290.

[6]. Wang, Q., Wang, B., Ma, Y., Zhang, X., Lyu, W., & Chen, M. (2022). Stabilization of heavy metals in biochar derived from plants in antimony mining area and its environmental implications. *Environmental Pollution, 300*, 118902.

[7]. Guo, P., Sun, F., & Han, X. (2023). Study on comprehensive evaluation of environmental pollution treatment effect in coal mine subsidence area: taking Xinglongzhuang mining area of Yanzhou energy as an example. *Environmental Science and Pollution Research, 30(3)*, 6132-6145.

[8]. Mutafela, R. N., Dahlin, T., Marques, M., & Hogland, W. (2020). Mapping and resource recovery process from heavy metal contaminated glass waste dumps. *Linnaeus Eco-Tech*.

[9]. Du, C., Wang, J., & Wang, Y. (2022). Study on environmental pollution caused by dumping operation in open pit mine under different factors. *Journal of Wind Engineering and Industrial Aerodynamics, 226*, 105044.

[10]. Seyedrahimi-Niaraq, M., Mahdiyanfar, H., & Mokhtari, A. R. (2022). Integrating principal component analysis and U-statistics for mapping polluted areas in mining districts. *Journal of Geochemical Exploration, 234*, 106924.

[11]. Chen, J., Yousefi, M., Zhao, Y., Zhang, C., Zhang, S., Mao, Z., ... & Han, R. (2019). Modelling ore-forming processes through a cosine similarity measure: Improved targeting of porphyry copper deposits in the Manzhouli belt, China. *Ore Geology Reviews*, *107*, 108-118.

[12]. Yilmaz, H., Yousefi, M., Parsa, M., Sonmez, F. N., & Maghsoodi, A. (2019). Singularity mapping of bulk leach extractable gold and− 80# stream sediment geochemical data in recognition of gold and base metal mineralization footprints in Biga Peninsula South, Turkey. *Journal of African Earth Sciences*, *153*, 156-172.

[13]. Zuo, R. (2011). Identifying geochemical anomalies associated with Cu and Pb–Zn skarn mineralization using principal component analysis and spectrum–area fractal modeling in the Gangdese Belt, Tibet (China). *Journal of Geochemical Exploration, 111(1-2)*, 13-22.

[14]. Afzal, P., Harati, H., Alghalandis, Y. F., & Yasrebi, A. B. (2013). Application of spectrum–area fractal model to identify of geochemical anomalies based on soil data in Kahang porphyry-type Cu deposit, Iran. *Geochemistry, 73(4)*, 533-543.

[15]. Mahdiyanfar, H. (2021). Prediction of economic potential of deep blind mineralization by Fourier transform of a geochemical dataset. *Periodico di Mineralogia, 90(1)*.

[16]. Shahi, H., Ghavami, R., Rouhani, A. K., Kahoo, A. R., & Haroni, H. A. (2015). Application of Fourier and wavelet approaches for identification of geochemical anomalies. *Journal of African Earth Sciences, 106*, 118-128.

[17]. Chen, G., & Cheng, Q. (2018). Fractal-based wavelet filter for separating geophysical or geochemical anomalies from background. *Mathematical Geosciences, 50(3)*, 249-272.

[18]. Shokouh Saljoughi, B., & Hezarkhani, A. (2019). Identification of geochemical anomalies associated with Cu mineralization by applying spectrum-area multi-fractal and wavelet neural network methods in Shahr-e-Babak mining area, Kerman, Iran. *Journal of Mining and Environment, 10(1)*, 49-73.

[19]. Parsa, M., Maghsoudi, A., Yousefi, M., & Sadeghi, M. (2017). Multifractal analysis of stream sediment geochemical data: Implications for hydrothermal nickel prospection in an arid terrain, eastern Iran. *Journal of Geochemical Exploration*, *181*, 305-317.

[20]. Ouchchen, M., Boutaleb, S., Abia, E. H., El Azzab, D., Miftah, A., Dadi, B., ... & Abioui, M. (2022). Exploration targeting of copper deposits using staged factor analysis, geochemical mineralization prospectivity index, and fractal model (Western Anti-Atlas, Morocco). *Ore Geology Reviews, 143*, 104762.

[21]. Mahdiyanfar, H., & Seyedrahimi-Niaraq, M. (2023). Integration of Fractal and Multivariate Principal Component Models for Separating Pb-Zn Mineral Contaminated Areas. *Journal of Mining and Environment, 14(3)*, 1019-1035.

[22]. Bazargani Golshan, M., Arian, M., Afzal, P., Daneshvar Saein, L., & Aleali, M. (2024). Outlining of High-quality Parts of Coal by Concentration–Volume Fractal Model in North Kochakali Coal Deposit, Central Iran. *Journal of Mining and Environment*, *15*(2), 557-579.

[23]. Afzal, P., Farhadi, S., Shamseddin Meigooni, M., Boveiri Konari,M, Daneshvar Saein, L., (2022). Geochemical Anomaly Detection in the Irankuh District Using Hybrid Machine Learning Technique and Fractal Modeling. *Geopersia, 12(1)*, 191-199.

[24]. Farhadi, S., Afzal, P., Boveiri Konari, M., Daneshvar Saein, L., Sadeghi, B., (2022). Combination of Machine Learning Algorithms with Concentration-Area Fractal Method for Soil Geochemical Anomaly Detection in Sediment-Hosted Irankuh Pb-Zn Deposit, Central Iran. *Minerals 12 (6)*, 689.

[25]. Merry, R. J. E. (2005). Wavelet theory and applications: a literature study.

[26]. Afzal, P., Ahmadi, K., & Rahbar, K. (2017). Application of fractal-wavelet analysis for separation of geochemical anomalies. *Journal of African Earth Sciences, 128*, 27-36.

[27]. Pourgholam, M. M., Afzal, P., Yasrebi, A. B., Gholinejad, M., & Wetherelt, A. (2021). Detection of geochemical anomalies using a fractal-wavelet model in Ipack area, Central Iran. *Journal of Geochemical Exploration, 220*, 106675.

[28]. Shokouh Saljoughi, B., & Hezarkhani, A. (2019). Identification of geochemical anomalies associated with Cu mineralization by applying spectrum-area multi-fractal and wavelet neural network methods in Shahr-e-Babak mining area, Kerman, Iran. *Journal of Mining and Environment, 10(1)*, 49-73.

[29]. Saljoughi, B. S., & Hezarkhani, A. (2020). Delineation of Alteration Zones Based on Wavelet Neural Network (WNN) and Concentration–Volume (CV) Fractal Methods in the Hypogene Zone of Porphyry Copper Deposit, Shahr-e-Babak District, SE Iran. *Journal of Mining and Environment, 11(4*), 1173-1190.

[30]. Pathak, R. S. (2009). The wavelet transform (Vol. 4). Springer Science & Business Media.

[31]. Shahi, H., Ghavami, R., & Rouhani, A. K. (2016). Comparison of mineralization pattern of geochemical data in spatial and position-scale domain using new DWT-PCA approach. *Journal of the Geological Society of India, 88*, 235-244.

[32]. Rhif, M., Ben Abbes, A., Farah, I. R., Martínez, B., & Sang, Y. (2019). Wavelet transform application for/in non-stationary time-series analysis: A review. *Applied Sciences, 9(7)*, 1345.

[33]. Akujuobi, C. M. (2022). Wavelets and wavelet transform systems and their applications. Berlin/Heidelberg, Germany: Springer International Publishing.

[34]. Vahedi, R., B. Tokhmechi, and M. Koneshloo. (2016). Permeability upscaling in fractured reservoirs using different optimized mother wavelets at each level. *Journal of Mining and Environment, 7(2)*, 239-250.

[35]. Tokhmechi, B., Rabiei, M., Azizi, H., & Rasouli, V. (2018). A new 2D block ordering system for wavelet-based multi-resolution up-scaling. *Journal of Mining and Environment, 9(4)*, 817-828.

[36]. Lotfi, M., & Tokhmechi, B. (2019). Fractal-wavelet-fusion-based re-ranking of joint roughness coefficients. *Journal of Mining and Environment, 10(4)*, 1121-1133.

[37]. Liu Y, Song Y, Fard M, Zhou L, Hou Z, Kendrick MA., (2019). Pyrite Re-Os age constraints on the Irankuh Zn-Pb deposit, Iran, and regional implications. *Ore Geology Reviews, 1(104)*, 148-59.

[38]. Ahankoub M, Asahara Y, Tsuboi M., (2020). Petrology and geochemistry of the Lattan Mountain

magmatic rocks in the Sanandaj–Sirjan Zone, west of Iran. *Arabian Journal of Geosciences, 13(16)*, 1-3.

[39]. Karimpour, M.H. and Sadeghi, M., (2018). Dehydration of hot oceanic slab at depth 30–50 km: KEY to formation of Irankuh-Emarat PbZn MVT belt, Central Iran. *Journal of Geochemical Exploration, 194,* 88–103.

[40]. Hosseini-Dinani H, Aftabi A, Esmaeili A, Rabbani M., (2015). Composite soil-geochemical halos delineating carbonate-hosted zinc–lead–barium mineralization in the Irankuh district, Isfahan, west-central Iran. *Journal of Geochemical Exploration. 1(156*), 114-30.

[41]. Mirghaffari N., (2005). Lead concentration in some natural plant species around the Irankuh lead and zinc mine in Isfahan. *Iranian J Nat Resour, 58*, 635–44. (in Persian).

[42]. Geranian, H., Mokhtari, A. R., & Cohen, D. R., (2013). A comparison of fractal methods and probability plots in identifying and mapping soil metal contamination near an active mining area, Iran. *Science of the total environment, 463*, 845-854.

[43]. Ghazifard A, Sharief M., (2003). The study of the extent of heavy metal absorption by agricultural crops and investigating its environmental contamination around Irankuh Pb and Zn deposit. *Isfahan Univ Res J, 17*, 153–66. (in Persian).

[44]. Mokhtari AR, Rodsari PR, Cohen DR, Emami A, Bafghi AA, Ghegeni ZK., 2015. Metal speciation in agricultural soils adjacent to the Irankuh Pb–Zn mining area, central Iran. *Journal of African Earth Sciences. 1(101),* 186-93.

[45]. Johansson, E. (2005). Wavelet Theory and some of its Applications, Department of Mathematics. *Lulea, Sweden, Lulea University of Technology*. Licentiate: 90.

[46]. Mertins, A. (1999). Signal Analysis: Wavelets, Filter Banks, Time-Frequency Transforms and Applications. *John Wiley & Sons*.

[47]. Bessissi, Z., Terbeche, M., Ghezali, B. (2009). Wavelet application to the time series analysis of DORIS station coordinates. *Comptes Rendus Geoscience, 341(6)*, 446-461.

[48]. Vetterli, M,. Kovacevic, J. (2007). Wavelets And Subband Coding, USA, New Jersey , Prentice Hall PTR, Englewood Cliffs.

[49]. Zhang, L., Bai, G., & Zhao, Y. (2012). A method for eliminating caprock thickness influence on anomaly intensities in geochemical surface survey for hydrocarbons. *Mathematical Geosciences*, *44*, 929-944.

[50]. Van Fleet, P. J. (2019). Discrete wavelet transformations: An elementary approach with applications. *John Wiley & Sons*.

[51]. Seo, Y., Kim, S., Kisi, O., & Singh, V. P. (2015). Daily water level forecasting using wavelet decomposition and artificial intelligence techniques. *Journal of Hydrology, 520*, 224-243.

[52]. Lindfield, G., & Penny, J. (2019). Chapter 8-Analyzing Data Using Discrete Transforms. Numerical Methods (Fourth Edition), *G. Lindfield and J. Penny, Eds*, 383-431.

[53]. Stanković, R. S., & Falkowski, B. J. (2003). The Haar wavelet transform: its status and achievements. *Computers & Electrical Engineering, 29(1)*, 25-44.

[54] Felja, M., Bencheqroune, A., Karim, M., & Bennis, G. (2023). The Effectiveness Daubechies Wavelet and Conventional Filters in Denoising EEG Signal. *International Conference on Digital Technologies and Applications*, 991-999.

[55]. Bahri, S., Awalushaumi, L., & Susanto, M. (2018). The approximation of nonlinear function using daubechies and symlets wavelets. *First International Conference on Mathematics and Islam*, 300-306.

[56]. Torshizian, H., Afzal, P., Rahbar, K., Yasrebi, A. B., Wetherelt, A., & Fyzollahhi, N. (2021). Application of modified wavelet and fractal modeling for detection of geochemical anomaly. *Geochemistry, 81(4)*, 125800.

[57]. Ge, H., Sun, Z., Lu, X., Jiang, Y., Lv, M., Li, G., & Zhang, Y. (2024). THz spectrum processing method based on optimal wavelet selection. *Optics Express, 32(3)*, 4457-4472.

[58]. Bølviken, B., Stokke, P., Feder, J. and Jössang, T. (1992). The fractal nature of geochemical landscapes. *Journal of Geochemical exploration, 43*, 91-109.

[59]. Cheng, Q., Agterberg, F. and Ballantyne, S. (1994). The separation of geochemical anomalies from background by fractal methods. *Journal of Geochemical Exploration, 51*, 109-130.

[60]. Lima, A., De Vivo, B., Cicchella, D., Cortini, M. and Albanese, S. (2003). Multifractal IDW interpolation and fractal filtering method in environmental studies: an application on regional stream sediments of (Italy), *Campania region. Applied geochemistry, 18*, 1853-1865.

[61]. Yousefi, M., & Carranza, E. J. M. (2015). Prediction–area (P–A) plot and C–A fractal analysis to classify and evaluate evidential maps for mineral prospectivity modeling. *Computers & Geosciences*, *79*, 69-81.

[62]. Paravarzar, S., Mokhtari, Z., Afzal, P., & Aliyari, F. (2023). Application of an approximate geostatistical simulation algorithm to delineate the gold mineralized zones characterized by fractal methodology. *Journal of African Earth Sciences*, *200*, 104865.

[63]. Zuo, R., Cheng, Q. and Xia, Q. (2009). Application of fractal models to characterization of vertical distribution of geochemical element concentration. *Journal of Geochemical Exploration, 102*, 37-43.

[64]. Madani, N. and Sadeghi, B. (2019). Capturing Hidden Geochemical Anomalies in Scarce Data by Fractal Analysis and Stochastic Modeling. *Natural Resources Research, 28*, 833-847.

[65]. Ghaeminejad, H., Abedi, M., Afzal, P., Zaynali, F., & Yousefi, M. (2020). A fractal-based outranking approach for integrating geochemical, geological, and geophysical data. *Bollettino Di Geofisica Teorica Ed Applicata*, *61(4)*, 555-588.

[66]. Mahdiyanfar, H., & Seyedrahimi-Niaraq, M. (2022). Improvement of geochemical prospectivity mapping using power spectrum–area fractal modelling of the multi-element mineralization factor (SAF-MF). *Geochemistry: Exploration, Environment, Analysis*, *22(4)*, geochem2022-015.

[67]. Seyedrahimi-Niaraq, M., & Hekmatnejad, A. (2021). The efficiency and accuracy of probability diagram, spatial statistic and fractal methods in the identification of shear zone gold mineralization: a case study of the Saqqez gold ore district, NW Iran. *Acta Geochimica*, *40*, 78-88.

[68]. Seyedrahimi-Niaraq, M., Mahdiyanfar, H., & Mokhtari, A. R. (2023). Application of geochemical structural methods to determine lead-contaminated areas related to mining activities. *Journal of Analytical and Numerical Methods in Mining Engineering, 13(34)*, 41-55.

کاربرد روش ترکیبی موجک-فرکتال برای نویززدایی و مدل‌سازی فضایی آلودگی محیطی

حسین مهدیانفر[۱] و میرمهدی سیدرحیمی‌نیارق[۲*]

۱. گروه مهندسی معدن، مجتمع آموزش عالی گناباد، گناباد، ایران

۲. دانشیار گروه مهندسی معدن، دانشکدهٔ فنی و مهندسی، دانشگاه محقق اردبیلی، اردبیل، ایران

ارسال ۲۰۲۴/۰۲/۱۵، پذیرش ۲۰۲۴/۰۵/۰۶

* نویسنده مسئول مکاتبات: m.seyedrahimi@uma.ac.ir

چکیده:

در این تحقیق از روش ترکیبی تبدیل موجک و روش فرکتالی به نام مدل موجک - فرکتال، به عنوان یک روش جدید، برای به نقشه در آوردن آلودگی ژئوشیمیایی استفاده شده است. برای این منظور، نقشه های توزیع عناصر آلاینده با استفاده از تبدیل موجک گسسته دو بعدی (2DDWT) به حوزه مقیاس موقعیت تبدیل شد. موجک مادر Symlet2 و Haar برای آنالیز سیگنال دو بعدی غلظت عنصری As، Pbو Zn بر اساس نمونه‌های خاک برداشت‌شده از منطقه معدنی ایرانکوه، ایران مرکزی استفاده شد. ضرایب موجک Symlet2 و Haar از اجزای تقریبی و جزئیات در تجزیه فرکانس یک سطح با استفاده از 2DDWT به دست آمد. ضرایب موجک مولفه تقریبی (WCAC) با استفاده از روش فرکتالی برای تعیین جوامع آلودگی ژئوشیمیایی عناصر سمی مدل‌سازی شد. بر اساس نتایج مدل‌های موجک-فرکتال، As، Pbو Zn به سه و چهار جمعیت طبقه‌بندی شدند. در این ناحیه، دو منطقه آلوده به فلزات پیدا شده است. این مناطق در محدوده عملیات معدنی و اطراف آن قرار دارند. مدل پیشنهادی موجک - فرکتال توانسته مناطق محیطی آلوده به فلزات سمی را به دقت جدا کند. آلودگی با آنومالی شدید تا یک کیلومتر خارج از محدوده عملیات معدنی گسترش یافته است. این پراکندگی در مورد عناصر سرب و روی در نقشه ژئوشیمیایی تهیه شده با کلاس ها به خوبی دیده می‌شود.

کلمات کلیدی: تبدیل موجک، موجک Symlet، موجک Haar، فرکتال عیار - مساحت، مدل موجک - فرکتال، آلودگی محیطی.